'Copenhagen Offshore Wind 2005'
Topic: Wind turbine technology - for offshore application. Wind resources and wake effects
Short-term forecasting of wind speeds in the offshore environment

Rebecca Barthelmie
Wind Energy Department, Risø National Laboratory, 4000 Roskilde, Denmark
Tel: +45 46775020, Fax: +45 46775970, email: r.barthelmie@risoe.dk

Gregor Giebel
Wind Energy Department, Risø National Laboratory, 4000 Roskilde, Denmark
Tel: +45 46775095, Fax: +45 46775970, email: gregor.giebel@risoe.dk

Jake Badger
Wind Energy Department, Risø National Laboratory, 4000 Roskilde, Denmark
Tel: +45 46775094, Fax: +45 46775970, email: jake.badger@risoe.dk

Summary

This paper focuses on a number of special issues that arise in terms of forecasting power output from large offshore wind farms. The effects considered are: wind speed gradients in the coastal zone and vertical wind speed profile extrapolation to hub-height. Wake effects are important but not considered here. Typically wind speed predictions for a specific location from a national weather service model are obtained and the local influences on the wind speed (orography, roughness changes etc) are applied using either physical or statistical approaches. Large offshore wind farms cover areas ~20 km^2 and so a gradient of wind speeds may need to be applied across the wind farm in order to capture the spatial variability. Additionally, short-term variations in stability can lead to the wind speed profile deviating from a logarithmic profile giving large errors in predicted wind speeds at turbine hub-heights.

Introduction

Wind resources in the coastal zone ought to be relatively easy to predict due to the lack of topography and obstacles, but a mesoscale model study of the Baltic Sea illustrated that topography, roughness change and temperature/humidity fluxes all had about an equal effect on wind resources at a specific site (10%) [1]. Roughness is much lower offshore (~0.0002 m) but is also dependent on wind speed. Strong gradients of temperature and humidity affect the distance over which the wind recovers to its offshore value and also impact the wind speed profile. Mesoscale circulations such as sea breezes [2], low level jets [3] and roll circulations [4] also impact the wind and turbulence experienced by wind turbines in coastal areas. To date, one of the biggest issues has been the relative lack of observations offshore, especially to turbine hub-heights.

In this paper we use a new approach to classify stability based on wind shear as forecast in HIRLAM. The stability correction was used to with 10 m forecast winds to predict wind speeds at 70 m and then compared with power output as observed at the Middelgrunden wind farm in Copenhagen. Mesoscale modelling was used to investigate whether stability has an impact on wind speed gradients at the Nysted offshore wind farm.

Atmospheric stability

Atmospheric stability describes the stratification of the atmosphere and the exchange of momentum downwards towards the surface. The standard method of describing stability is to use the Monin-Obukhov length, which is the ratio of mechanically generated to buoyancy generated turbulence:

$$L = -\left(\overline{u'w'}^2 + \overline{v'w'}^2\right)^{3/4} / \left(\kappa(g/\overline{\theta_v})(\overline{w'\theta_v'})\right) \quad (1)$$

When L > 0 conditions are stable implying limited energy transfer, when L < 0 conditions are unstable (convective) and when | L | > 1000 conditions are close to neutral. Once L has been defined corrections can be calculated to the logarithmic profile.

$$U_z = \frac{u_*}{\kappa}\left[ln\frac{z}{z_0} - \Psi_m\left(\frac{z}{L}\right)\right] \quad (2)$$

If conditions are stable:

$$L > 0 \quad \Phi_m = \frac{\kappa z}{u_*}\left[\left(\frac{\partial \overline{U}}{\partial z}\right)^2 + \left(\frac{\partial \overline{V}}{\partial z}\right)^2\right]^{1/2} = 1 + 4.7\frac{z}{L} \quad (3)$$

$$\Psi\left(\frac{z}{L}\right) = \frac{4.7z}{L} \quad (4)$$

and if they are unstable:

$$L < 0 \quad \Phi_m = \frac{\kappa z}{u_*}\left[\left(\frac{\partial \overline{U}}{\partial z}\right)^2 + \left(\frac{\partial \overline{V}}{\partial z}\right)^2\right]^{1/2} = \left(1 - 15\frac{z}{L}\right)^{-1/4} \quad (5)$$

$$\Psi\left(\frac{z}{L}\right) = -2ln\left[\frac{(1+x)}{2}\right] - ln\left[\frac{\left(1+x^2\right)}{2}\right] + 2tan^{-1}(x) - \frac{\pi}{2} \quad (6)$$

$$where\ x = \left[1 - (15z/L)\right]^{-1/4} \quad (7)$$

The reason that stability appears to be more important offshore is that on average mechanically generated turbulence is low due to the low roughness of the sea surface. In contrast to land surfaces where temperatures vary significantly between day and night, the sea surface temperature is relatively constant at this time scale. Changes in sea surface temperature typically lag changes in air temperature from nearby land by about one month. This gives rise to large temperature gradients in coastal areas which are most pronounced in spring and autumn. It is also worth noting that stability appears to be mainly synoptic with a small influence of the fetch [5]. This means that stability varies little on the diurnal timescale but that there are pronounced seasonal differences with a higher number of stable conditions in spring (Figure 1).

Wind speed profiles

Previous work has shown that stability corrections are necessary in order to accurately capture the wind speed gradient with height. As shown in Figure 2 stability corrections increase with height therefore they become important as wind turbine hub-heights increase. Furthermore, the wind shear over the rotor diameter depends on stability. One of the difficulties in applying stability corrections to offshore wind speed profiles is that lack of accurate temperature gradient measurements (assuming flux measurements from a sonic anemometer are not available). As has been shown [5], [6] the choice of temperature measurements strongly impacts the outcome. Here we use a new method based on the wind shear from the HIRLAM model in order to avoid problems associated with temperature measurements. The site is an offshore location close to the Middelgrunden wind farm (Figure 3).

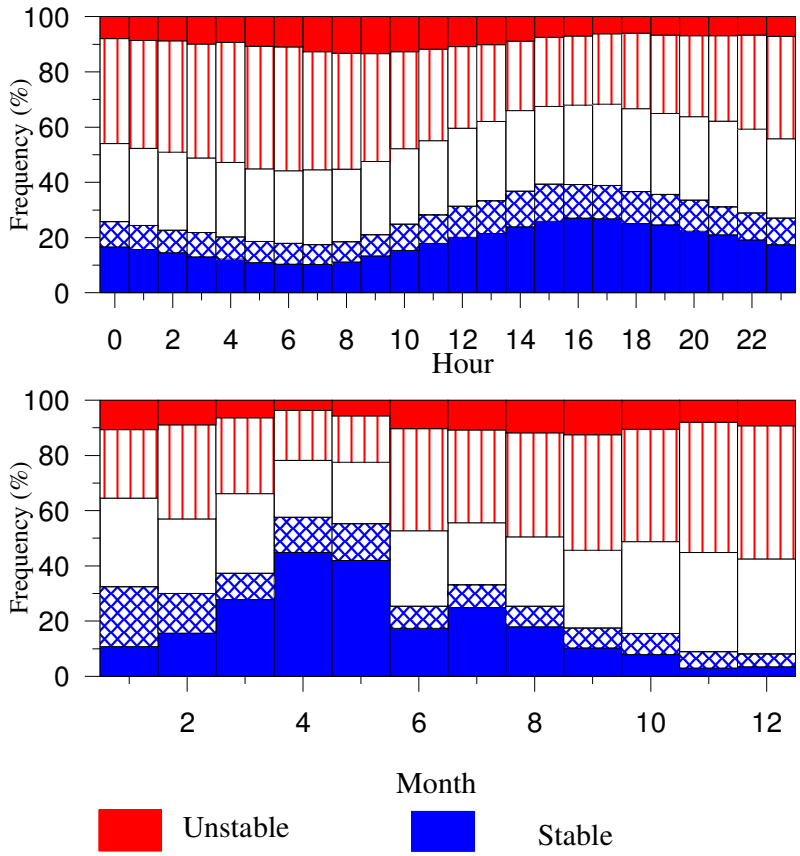

Figure 1. Frequency of stability conditions for a Danish offshore site (top by hour and bottom by month).

For an overview of HIRLAM prediction of short-term wind speeds see e.g. [7].The Monin-Obukhov length (L) is approximated based on the wind shear between wind speeds at 10 m and the different model levels. Model levels are calculated assuming hydrostatic equilibrium:

$$\Delta z = -\frac{\Delta P}{\rho g} \tag{8}$$

where z is height
ρ is air density
g is acceleration due to gravity
P is pressure

The method assumes that the 10 m wind speed and one other model level will be available.

- Wind speeds less than 1 m/s at the model level are discarded
- Wind speeds above 15 m/s at the model level are assumed to be near-neutral
- If the absolute difference between the model level wind speed and the log. predicted wind speed is greater than 5% then conditions are assumed to be non-neutral.
- If the difference is positive – conditions are assumed to be stable, if it is negative conditions are assumed to be unstable.

First the difference between the predicted wind speed based on the logarithmic profile and the 10 m wind speed and the wind speed at the model level is calculated. For the stable case, the correction to the logarithmic profile is straightforward [8]:

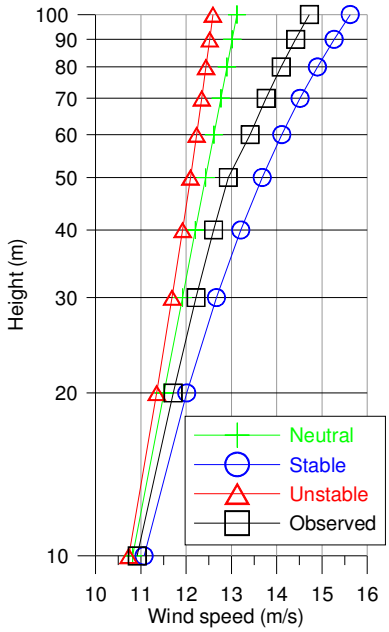

Figure 2. Illustration of stability impacts on wind speed profiles according to equations 2-7.

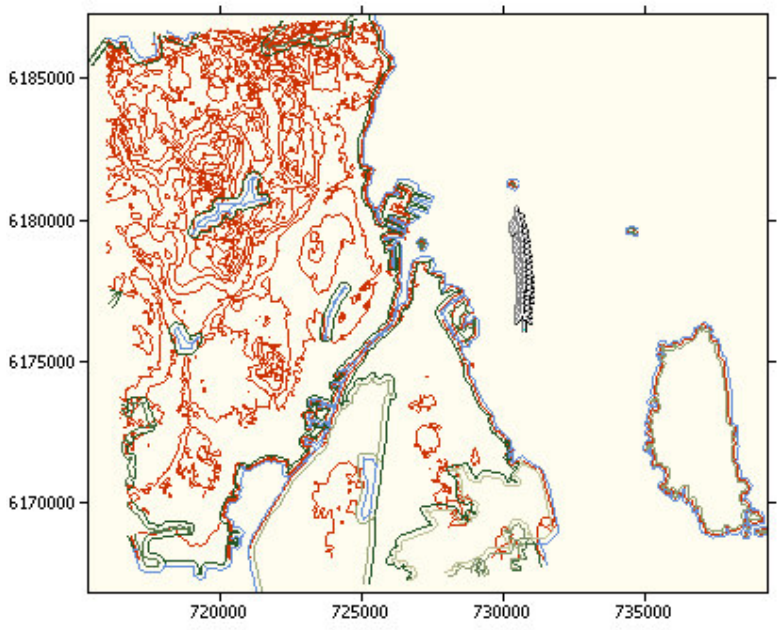

Figure 3. Location of the Middelgrunden wind farm near Copenhagen. Lines show contour levels. Coordinates are UTM zone 32.

$$Uz = \frac{u_*}{k}\left(ln\frac{z}{z_0} + 4.7\frac{z}{L} \right) \tag{9}$$

and L is estimated based on the difference between wind speeds at the model level and 10 m. Given the complexity of the unstable correction (see e.g. [8]), a simpler solution was found which was to apply two polynomial fits to the correction versus the Monin-Obukhov length. For profile corrections between 0.1 and 0.5 m/s, the Monin-Obukhov length is estimated using a fifth degree polynomial

while for profile corrections between 0.5 and 2 m/s, the Monin-Obukhov length is estimated using a third degree polynomial. Once L is determined, the stability corrected wind speed at hub-height (here set to 70 m) can be determined using equation (2). Power output is estimated using a polynomial fit to the power curve between 4 and 15 m/s. Power output is set to zero if the wind speed is below 4 m/s or above 25 m/s and to 2 MW if the wind speed is between 17 and 25 m/s. As shown in Figure 4 and 5, the power output estimated from the stability corrected wind speed at hub-height is typically but not always higher than the power estimate from the logarithmic prediction.

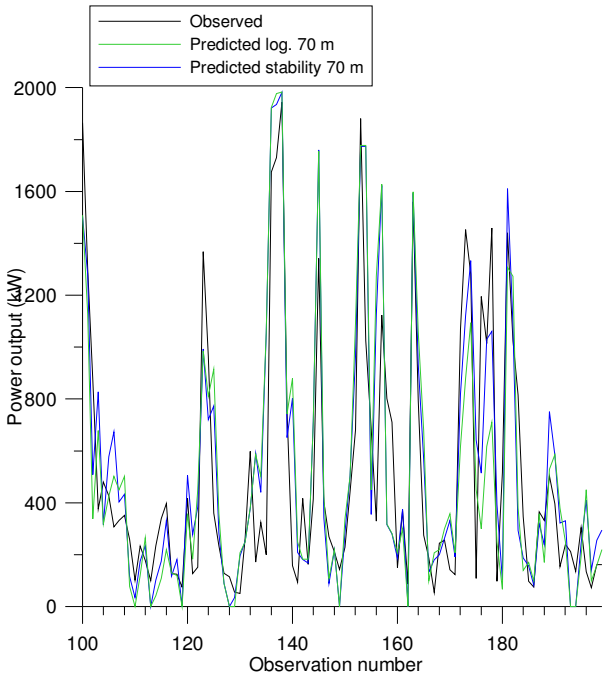

Figure 4. Measured/modelled power output for Middelgrunden for a set of observations in the middle of the data period (shown for hour zero).

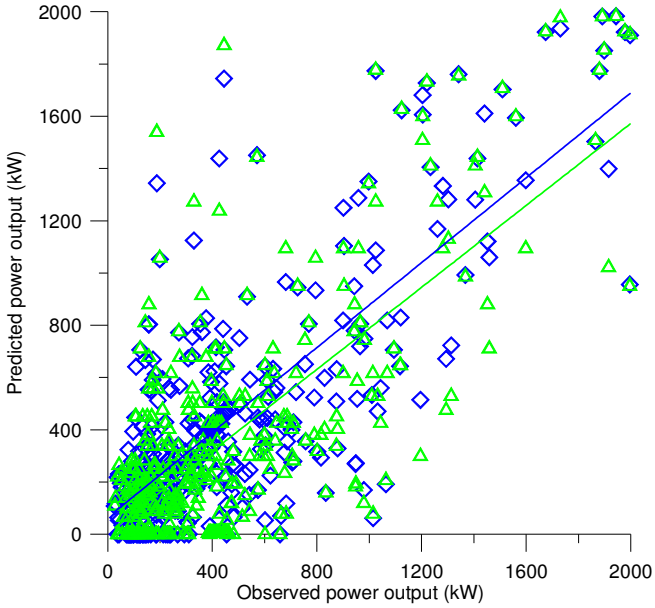

Figure 5. Comparison of observed and predicted power output for one turbine at Middelgrunden.

The next step is to evaluate whether the predicted wind speeds using this method are more accurate in comparison to the power output at Middelgrunden. Here we use data from the Middelgrunden wind farm where the observed power is from the north or south turbine selected by direction. The overlap with the available HIRLAM data give a test dataset of 351 observations mainly from the summer months of 2001 and 2002. As shown in Figure 6, the use of the prediction with the stability correction gives slightly higher power output than the use of the logarithmic prediction. In order to evaluate the short-term forecasts over 48 hours, the power output is calculated using the 10 m forecast wind speed and either the log. profile or the stability corrected profile where the stability correction is calculated for hour zero and then applied to the subsequent 48 hours (Figure 6). A bias of 0.5 m/s was added to the HIRLAM 10 wind speed from which both were calculated.

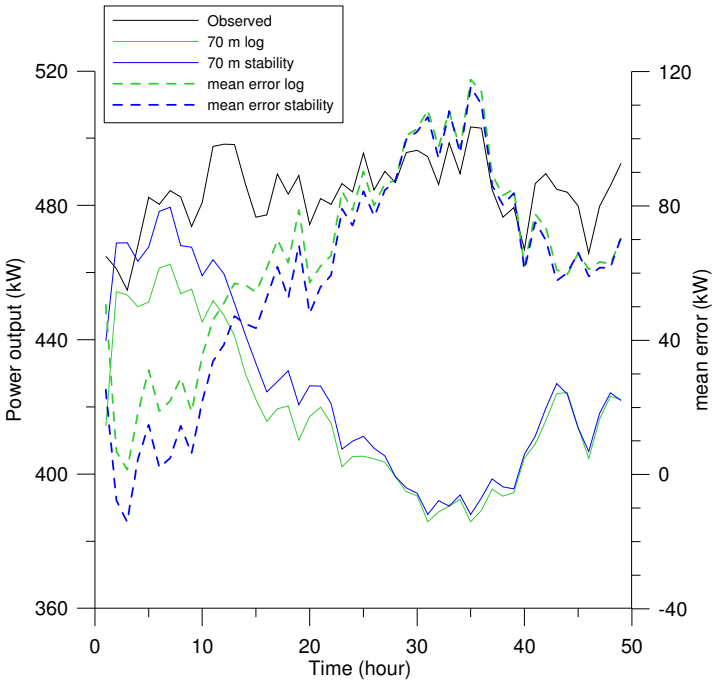

Figure 6. 48 hour observed and predicted power output for a turbine at Middelgrunden (average of 351 test cases.

Wind speed gradients: Mesoscale modelling for Nysted

The Karlsruhe Atmospheric Mesoscale Model (KAMM, [10]) is used extensively in wind energy applications [11]. Here KAMM is used in a idealized way to investigate the effects of regional topography and surface temperature differences over land and sea on winds around the Nysted wind farm. This is done by integrating the model using a set of 12 wind forcing directions for various surface temperature configurations. The KAMM modelling was performed on a 5 km resolution 200x200 km domain centred on the Nysted wind farm. The upper boundary was set to 5500 m above sea level with 25 model levels. Non-uniform spacing concentrates more levels at the lower heights. KAMM requires a potential temperature and geostrophic wind speed and direction profile to define the forcing state of the model which were calculated using NCEP/NCAR reanalysis data for the four nearest grid points to the wind farm for years 1965 to 1998 at heights 0 m, 1500 m, 3000 m and 5500 m above sea level (Figure 8). The mean geostrophic wind at 0 m is 9.826 m/s. To simplify the profile, the mean winds at all heights were multiplied by 10.0/9.826 to give a 10 m/s geostrophic forcing at 0 m and the correct wind shear. Figure 7 shows the potential temperature and wind speed profiles used for the KAMM modelling. The mean geostrophic wind directions for the 4 heights are 262^{o}, 268^{o}, 272^{o}, 275^{o}, indicating a turning of the geostrophic wind and warm advection. In this idealized study a

set of 12 wind directions was used from 0° to 330° with a constant 30° interval and no variation of direction with height.

In KAMM the land and sea surface temperatures can be set by a constant offset relative to the lowest model level air temperature at initialization. In the first set of integrations, set A, the offset temperature is set to 0K for both land and sea surfaces ie. the surface temperature is set to the lowest model level air temperature at initialization everywhere in the domain and does not change during the model integration. In the second set of integrations, set B, the surface temperature offset is +5K for sea surfaces and –5K for land surfaces ie. sea surface is warm and the land surface is cold. In the third set of integrations, set C, the surface temperature offset is –5K for sea surfaces and +5K for land surfaces, meaning a cold sea surface and a warm land surface. The temperature differences are higher than those typically experienced at coastal locations in Denmark.

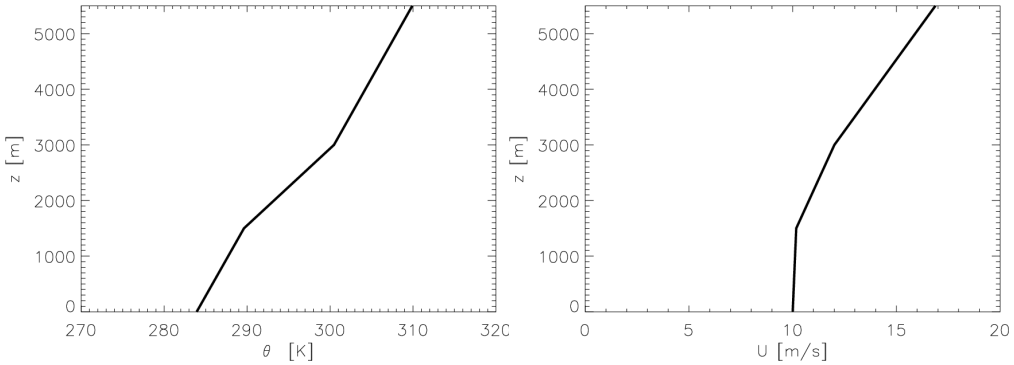

Figure 7. Graphs showing the potential temperature (θ) profile (left) and wind speed profile (right) used in the KAMM simulations.

Figure 8 shows the wind vector for the 90° wind forcing at 70 m above surface level after a 6 hour integration. In the area around the Nysted wind farm the wind speed increases as changes to the boundary layer take place after the abrupt reduction in surface roughness from land to sea. The variation of wind speed and direction experienced over the extent of the wind farm is influenced by large-scale wind forcing and surface temperature conditions. Figure 9 shows the wind speed and direction at 70 m for the 4 corners of the wind farm as a function of wind forcing angle for simulations from set A. It shows that the wind speed varies with wind forcing angle with two relative maxima for wind speed occurring at 90° and 240° forcing angle. These directions correspond to north-easterly and south-westerly winds respectively at the wind farm. In these directions there is a long fetch to southern Sweden. Two relative minima of wind speed occur on Figure 9 at around 330° - 30°, 150° wind forcing angle. These directions correspond to north-westerly to northerly and south-easterly winds respectively at the wind farm at 70 m. In these directions, especially north-westerly to northerly, the sea fetch is short.

Figure 9 also shows that there is variation of wind speed within the extent of the wind farm. Agreement between the grid points is best for wind directions ranging from southerly to south-westerly. Agreement is worst for wind directions ranging from westerly to easterly. This can be understood in terms of the complexity of nearby coastline; greatest variation of wind speeds is seen when the wind is blowing from a nearby coastline. From Fig. 9 it can be seen that the wind direction does not vary greatly within the wind farm. The offset between the wind forcing angle and the wind direction at 70m is greatest for the wind forcing angle of 150° and smallest for the wind forcing angle of 300°. Figures 10 and 11 show the wind speed and direction variation within the farm and as a function of wind forcing angle for simulations from set B and C.

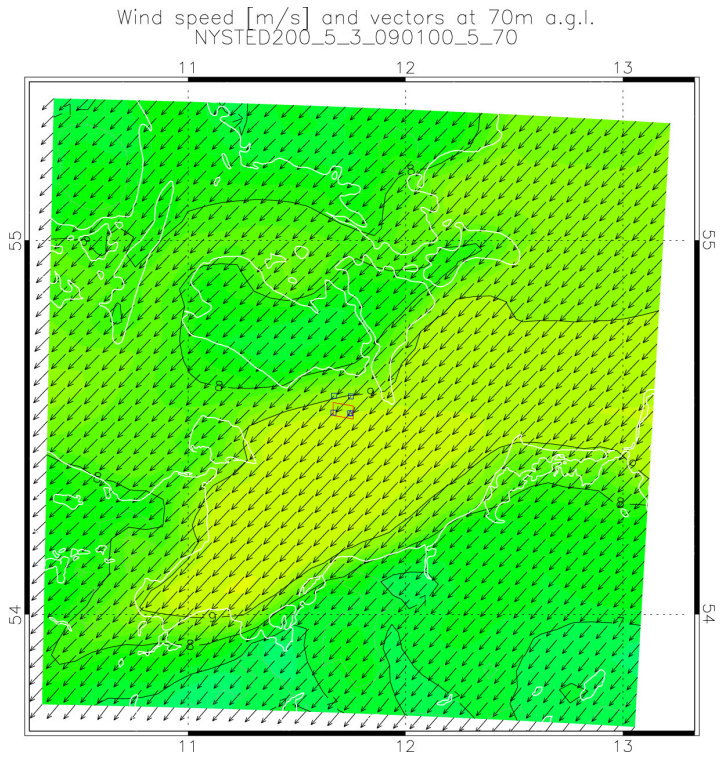

Figure 8. The wind field at 70 m above the surface for the configuration used in set A (see main text for details) for the 90° wind forcing. The small red rhomboid and blue squares mark the extent of the Nysted wind farm and the closest KAMM grid points respectively.

For set B, warm sea – cold land, the variation of wind speed as a function of wind forcing angle is reduced compared to set A. The maxima and minima are approximately located at the same forcing angles. Also the variation within the wind farm is reduced, except in cases where the wind is blowing from the range north to northeast, off the nearby coastline. With a wind forcing angle of 60° there is also a variation of wind direction at 70 m. Above the warm sea surface, reduced stability increases the mixing of air with higher momentum from aloft. Conversely, above the cold land surface, increased stability decreases this mixing.

So generally the wind above land is reduced compared to set A, whereas the wind above sea is increased compared to set A. Therefore there is typically a more distinct and sharp change of wind speeds along the coastline, hence the variation in farm wind speeds when the wind is blowing off the nearby coastline, when the wind farm is partly within the sharp transition. On the other hand, the variation of wind speeds as a function of wind forcing angle is reduced because fetch plays a less important role when the marine boundary layer is unstable.

For set C, cold sea – warm land, the variation of wind speed as a function of wind forcing angle is greater compared to simulations from set A and B. Also the variation of wind speed within the wind farm is greater for most wind forcing angles. The wind directions at 70 m vary only slightly more than the simulations from set A.

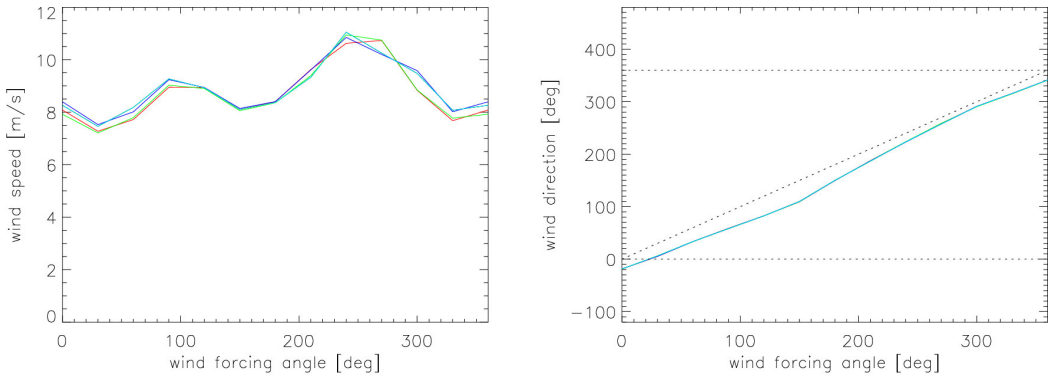

NYSTED200_5_3_000100_5_70

Figure 9. The wind speed (left) and direction (right) for the grid points nearest the corners of the Nysted wind farm (shown with different colours) as a function of large-scale wind forcing angle for the simulations of set A.

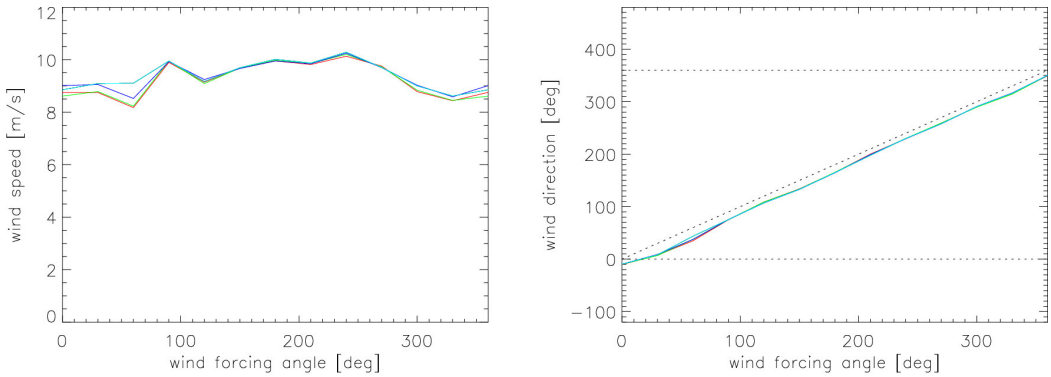

NYSTED200_5_4_000100_5_70

Figure 10. As in Fig. 9 except for the warm sea – cold land simulations of set B.

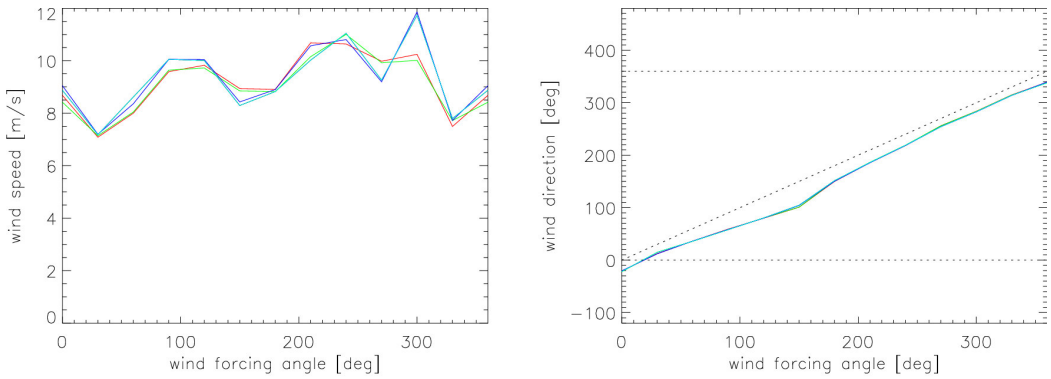

NYSTED200_5_5_000100_5_70

Figure 11. As in Fig. 9 except for the cold sea – warm land simulations of set C.

Explaining the wind characteristic of set C is more complicated. To start with, above a cool sea surface, increased stability decreases the mixing of air with higher momentum from aloft and may give rise to reduced wind speeds at low level. Conversely above the warm land increased mixing may give rise to increased wind speeds. In this case a less distinct pattern of winds above land and sea is formed at low levels, because of the stability is countering the roughness effects. However, for transitions to a stable marine boundary layer, jet features can arise caused by an imbalance of the pressure, Coriolis and frictional forces, following a decoupling of the frictional force due to an

increase in stability [1]. Such jet features can then give rise to increased winds above the cool sea. From the simulations of set C a mix of these effects is seen. For instance in some locations large wind shear is created between 25 m to 70 m above the sea surface, in other locations the 'wind shadow' of an island extends many tens of kilometres across the sea. This complexity is reflected in the large variations in wind speed within the farm and for different wind forcing angles in this set of simulations.

Summary

It has been shown that atmospheric stability continues to be an issue when calculating wind and turbulence at coastal sites. Stability is also known to impact wake losses although these results cannot be shown for reasons of commercial confidentiality. Although it is more difficult to implement procedures for short-term forecasting than for resource work, a new method has been described which attempts to classify stability based on wind shear alone. Preliminary results indicate that the method gives slight improvement of wind speed/power output although further evaluation is required. The relative lack of variation of stability on the diurnal timescale suggests that the stability correction can be approximated using a constant bias. However, the stability correction may need to vary at the seasonal time scale. Modelling of wind speed gradients at Nysted also show the importance of stability. In this case, stable conditions can lead to non-linear changes of the wind speed with distance from the coast.

Acknowledgements

This work was funded in part by the Danish Public Service Obligation (F&U4103), Danish Science and Technological Research Council (STVF 2104-04-0005) and the Anemos project (ENK5-CT-2002-00665) funded by the European Commission under the 5th (EC) RTD Framework Programme (1998 - 2002) within the thematic programme "Energy, Environment and Sustainable Development". Energi E2 kindly provided data from Middelgrunden. DMI is acknowledged for HIRLAM data.

References

[1] Bergström, H., 2002, Boundary-layer modelling for wind climate estimates, Wind Engineering, **25(5)**, 289-299.

[2] Borne, K., D. Chen, and M. Nunez, 1998, A method for finding sea breeze days under stable synoptic conditions and its application to the Swedish west coast, Int. J. Clim, **18**, 901-914.

[3] Smedman, A.S., U. Hogstrom, and H. Bergstrom, 1996, Low level jets - a decisive factor for off-shore wind energy siting in the Baltic Sea, Wind Eng, **20**(3), 137-147.

[4] Smedman, A.S., 1991, Occurrence of roll circulations in a shallow boundary layer., Boundary-Layer Meteor., **57**(4), 343-358.

[5] Motta, M., R.J. Barthelmie, and P. Vølund, 2005, The influence of non-logarithmic wind speed profiles on potential power output at Danish offshore sites, Wind Energy, **8**, 219-236.

[6] Barthelmie, R.J., 1999, The effects of atmospheric stability on coastal wind climates, Meteorological Applications, **6**(1), 39-48.

[7] Feddersen, H. and K. Sattler, Verification of wind forecasts for a set of experimental DMI-HIRLAM ensemble experiments. 2005, DMI sr05-01, Copenhagen, 15 pp.

[8] Stull, R.B., 1988, An introduction to boundary layer meteorology, ISBN 90-277-2768-6 ed, Kluwer Publications Ltd, Dordrecht, pp. 666.

[9] Barthelmie, R.J., G. Giebel, B. Jørgensen, J. Badger, S.C. Pryor, and C.B. Hasager. 2004, Comparison of corrections to site wind speeds in the offshore environment: value for short-term forecasting, EWEC, London, November 2004, 9 pp.

[10] Adrian, G. and F. Fiedler, 1991: Simulation of unstationary wind and temperature fields over complex terrain and comparison with observations. Beitr. Phys. Atmosph., **64**, 27-48.

[11] Frank, H.P. and L. Landberg, 1997. Modelling the wind climate of Ireland, Boundary-Layer Meteor., **85**, 359-387.